LARGE EDDY SIMULATION OF A SYMMETRIC BUMP ON STRUCTURED AND UNSTRUCTURED GRIDS, COMPARISONS WITH RANS AND T-RANS MODELS

Sofiane Benhamadouche
Département Mécanique des Fluides et Transferts Thermiques,
Electricité de France R&D,
6 quai Watier, Chatou, France
sofiane.benhamadouche@edf.fr

Juan Uribe, Nicolas Jarrin, Dominique Laurence
School of Mechanical, Aerospace and Civil Engineering,
The University Of Manchester,
Manchester, UK
j.uribe-2@postgrad.umist.ac.uk
N.Jarrin@postgrad.umist.ac.uk
dominique.laurence@manchester.ac.uk

ABSTRACT

One of the symmetric bumps available from the experiment of Simpson et al. (2002) is investigated in the present paper with various models. The Reynolds number based on the height of the hill and the maximum velocity at the inlet is 130 000. The unstructured collocated finite volume code *Saturne* is used for all the computations. Two RANS, a T-RANS and a Large Eddy Simulation (LES) calculation are first reported using a structured grid with about 900 000 cells. Both RANS models and LES fall in predicting the appropriate velocity profiles. T-RANS produces better results but still not the correct velocity field. Then, unstructured meshes using non-conforming faces are used for a better near wall resolution, with still less than a million cells. The obtained results are much better than in the previous simulations.

INTRODUCTION

Simpson et al. (2002) studied the boundary layer of the flow over several symmetrical bumps or hills and measured the 3D vortical separations behind the obstacles. These kinds of flows are very difficult to predict with turbulence models as reported in Wang et al. (2004). Indeed, this paper concludes that no turbulence model (even Large Eddy Simulation) managed to predict the present flow.

The 3D hill in the present paper (which corresponds to the bump #3 in Simpson's article) has been chosen in the framework of the European project FLOMANIA (Flow Physics Modelling – An Integrated Approach) and has been computed by several partners and with many turbulence models. As all RANS models (including Detached Eddy Simulation) and several LES failed to predict such a flow, the 3D hill has been kept as a crucial test-case in the framework of DESider (Detached Eddy Simulation for Industrial Aerodynamics) European project, the successor of FLOMANIA.

In the present work, several models are tested on structured grids. Then, after presenting the ability of code *Saturne*® (EDF's in-house finite-volume solver) to tackle local refinements and the capabilities of this method, Large Eddy Simulation is carried out on a fine grid with a reasonable number of cells.

TEST-CASE DESCRIPTION

The three-dimensional hill investgated in the present work is that from the experiments by Simpson et al. (2002) and Byun et al. (2004). The geometry of the computational domain is given in figure 1. The body height is $H=0.078$ *mm*. The geometry of the hill is given by the following function,

$$\frac{y(r)}{H} = -\frac{1}{6.04844}\left[J_0(\Lambda)I_0\left(\lambda\frac{r}{a}\right) - I_0(\Lambda)J_0\left(\lambda\frac{r}{a}\right)\right].$$

where $\Lambda=3.1962$ and $a=2H$. J_0 and I_0 are respectively the Bessel function of the first kind and the modified Bessel function of the first kind. The Reynolds number, based on the maximum inlet velocity ($U_{ref}=27.5$ *m/s* in the experiment) and the hill height H is $Re=130\,000$.

The Hill is placed at a distance $L_1=4$ *m* from the inlet and $L_2=8$ *m* from the outlet (see figure 1). The channel has two lateral walls with a distance $L_3=11.66$ *m* and a roof at height of $L_4=3.20513$ m from the ground plane.

The tunnel free-stream turbulent intensity reported in (Simpson *et al.*2002) is *0.1%*. The boundary layer when the hill was not in place was equal to *39 mm* at the position of the hill. All the variables in the present paper are normalized by H and U_{ref}.

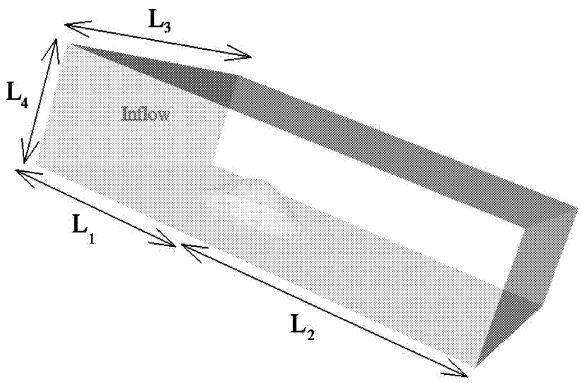

Figure 1: Computational domain definition

TURBULENCE MODELLING

Both RANS and LES approaches are used in the in-house EDF code *Saturne* (Archambeau et al. 2004). Briefly, *Saturne* is an unstructured collocated finite volume code using a SIMPLEC algorithm for pressure-velocity coupling with Rhie and Chow (1983) interpolation to avoid odd-even decoupling on structured meshes. The space discretisation is of second order using a gradient correction when needed on non-orthogonal faces. Both first order (implicit Euler) and second order (Crank-Nicolson and Adams Bashforth) time advancing schemes are available. All the models described herein are implemented in *Saturne*. Further references on the models and code are given in the two sections below..

RANS Approaches

Three different models are employed: the v2-f with the φ modifications (Laurence et al. 2003), the k-ω (Wilcox 1988) and the unsteady form of the classical LRR Reynolds Stress Model without wall echo terms (Launder et al. 1975). The first two are used on half of the geometry using the symmetry of the hill. This enforces the steady behaviour of the solution as all the computations use a time-dependant approach to solve Navier-Stokes equations. The last model is used on the full domain allowing an unsteady solution to develop. Time averaging is then performed on the velocity. The steady inlet conditions provided by the experimental data are used for all RANS simulations (including the unsteady one). The RANS computations were carried out with a CFL number of 1 and converged to a steady state.

LES Approach

Large Eddy Simulation has been successfully used in *Saturne* on academic or industrial cases (Benhamadouche et al. 2002, Benhamadouche and Laurence 2003, Benhamadouche et al. 2003). The approach has been developed in *Saturne* with a second order time advancing scheme based on a Crank-Nicolson time discretisation with an Adams-Bashforth scheme for the transporting velocity. Both the standard and the dynamic Smagorisky models are available but only the standard one is used in the present work with the Smagorinsky constant set to *0.065*. The vortex method presented in (Jarrin et al. 2003) is used to generate synthetic turbulence at the inlet. This method is flexible as it allows adding coherent fluctuations to a given mean velocity profile based on the velocity profile itself, the Reynolds Stresses and the dissipation.

USE OF NON-CONFORMING MESHES

When structured meshes are used, too many grid points might be generated and unfortunately a significant part of the nodes are located outside regions of interest. To have a proper refinement (particularly in the near-wall regions), structured meshes may entail several hundred of million nodes which is impossible to handle even with the most recent supercomputers.

To tackle this problem, it is possible with an unstructured approach that accepts cells of any shape, , to use hanging nodes (this approach will be called non-conforming approach in the framework of collocated finite volumes).

The channel flow at $Re^*=395$ is computed with both a structured mesh and a multi-block mesh with different levels of refinements (see figure 2). The computational domain is $2\pi \times 2 \times \pi$. The number of nodes in both cases is about *150 000* and no slip boundary conditions are used at the wall. Periodic boundary conditions are used in the streamwise and spanwise directions. The standard Smagorinsky subgrid scale model is used with the Smagorinsky constant set to *0.065*.

Figures 3 and 4 show the velocity profiles and the streamwise fluctuations compared to DNS results from Kim et al. (1987). Although approximately the same number of cells is used in both simulations, the non-conforming mesh exhibits obviously superior results. This is due to an appropriate refinement at the wall in the spanwise direction (of DNS order of magnitude, see figure 2). The computational cost is not dramatically increased. The reconstruction method at the non-conforming interfaces might increase the computational cost, in particular in the Poisson equation solver. As it can be seen in figure 4, the wall normal fluctuation matches exactly DNS results before the first interface of non-conforming faces. Between the first and the second interface, the mesh is finer than in the conforming case (structured mesh) particularly close to the wall and the amount of the simulated kinetic energy is higher than in the results with the structured mesh. Above the second interface, the cells on the non-conforming mesh are coarser than in the conforming one in order to keep approximately the same number of node. The amount of the computed energy is then lower than in the conforming mesh and this could be observed in figure 4.

However, it has been noticed that the use of this kind of refinement with interfaces orthogonal to the main flow in conjunction with a purely central difference scheme can generate artificial oscillations. That is why this technique of refinement will be used in the wall normal direction and in the streamwise direction in only in regions of lesser interest (in the 3D hill case, far downstream the bump after the plane of measurements $x=3.69$)

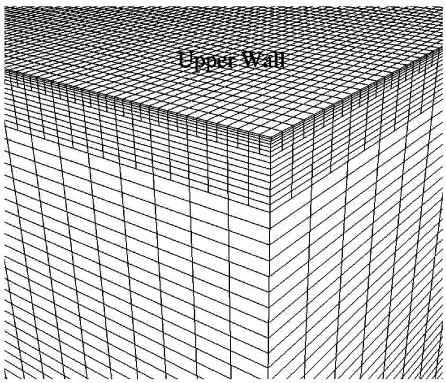

Figure 2: A non-conforming mesh (Channel flow)

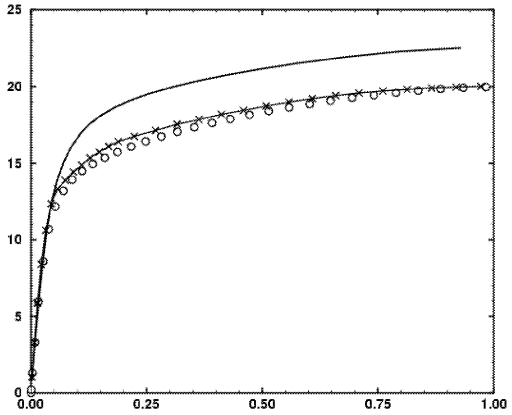

Figure 3: Velocity profiles (o DNS, x LES with non-conforming mesh, — LES with conforming mesh)

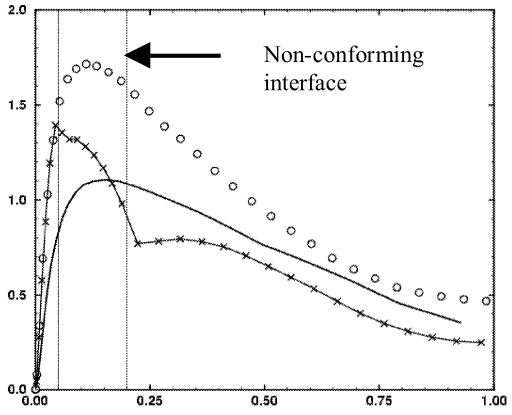

Figure 4: Wall normal fluctuations (o DNS, x LES with non-conforming mesh, — LES with conforming mesh)

NUMERICAL RESULTS ON THE 3D HILL

For the sake of clarity, the structured and unstructured results are presented separately.

Structured meshes

Structured meshes with about 880 000 nodes are used with RANS models and LES. The steady RANS models were computed on half of the domain using the symmetry of the hill to force the steady behavior with an unsteady algorithm.

Figures 5 and 6 give the streamwise velocity profile at two representative locations (the line $x=3.69$, $z = 0.08$ close to the symmetry plane and the line $x=3.69$, $z=0.8$ in a vortex normal to the streamwise direction) compared to the experimental results. As one can observe, neither steady RANS models nor LES give a satisfactory solution and predict a too long separation in the symmetry plane. The unsteady RANS model based on LRR approach gives much better results but still far from the experimental ones particularly close to the symmetry plane. Figure 7 exhibits the tangential velocity field in the plane of measurements $x=3.69$ for both the experiment and the unsteady RANS computations (just half of the plane is represented as the plane $z=0$ is a symmetry plane). The experiment records two counter-rotating vortices. In figure 6, the center of the vortex is located in the *(yz)* plane around the point (0.25; -1.4) for the experimental results. The unsteady RANS computation predicts two counter-rotating vortices located respectively at (0.19, -0.54) and (0.21, -1.28). The second vortex corresponds to the experimental one but is obviously less energetic (in figure 7, the scale of the velocity vectors has been doubled for unsteady RANS simulation). The first vortex is much more energetic but has no physical justification.

As it has been shown in Wang et al. (2004), no model on structured meshes is able to predict the 3D hill flow correctly. As the Reynolds number is quite high for a reasonable Large Eddy Simulation with a structured approach, the mesh has to be finer at the wall than the structured one used herein. If a structured approach is kept, several millions of nodes would be needed for a reasonable resolution. As this order of magnitude is still unaffordable, an unstructured approach based on the use of hanging nodes (non-conforming meshes) is presented. Almost the same number of cells will be used than in the structured case.

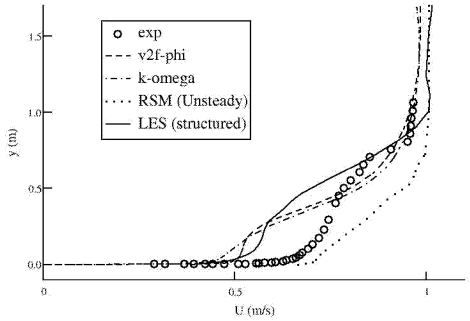

Figure 5: Streamwise velocity profile ($x=3.69$, $z = 0.08$)

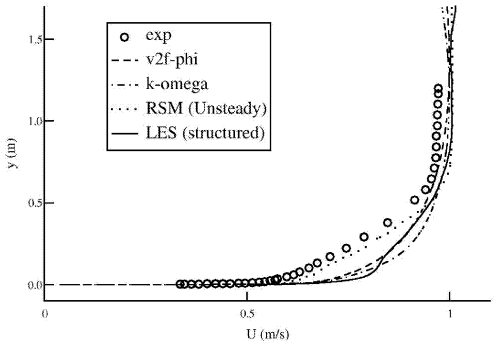

Figure 6: Streamwise velocity profile ($x=3.69$, $z = 0.8$)

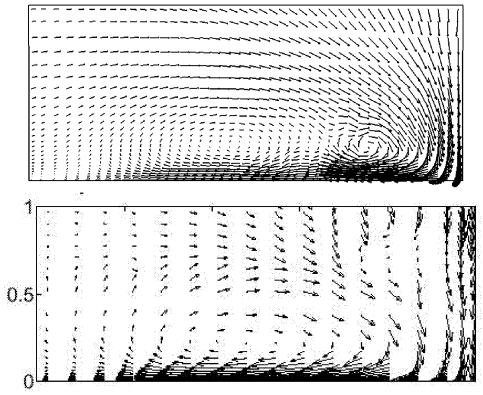

Figure 7: Tangential velocity field in the plane $x=3.69$ (top: Unsteady LRR (scale x2), bottom: experiment)

Unstructured meshes

The mesh contains about 900 000 cells. No slip boundary conditions are used at the wall and a vortex method (Jarrin et al. 2003) based on the experimental velocity and Reynolds stresses profiles is imposed at the inlet. The side walls are not taken into account and symmetry boundary conditions are imposed as the mesh is very coarse at that location and this walls should not have an influence on the flow around the 3D hill. The time step is set to 0.002 what gives a maximum Courant number of *0.3*. The averaging is performed over 5 flow-through passages which as one will see, is not enough to obtain a fully converged solution.

Figures 8 and 9 show the non-conforming mesh used herein. The upper half of the channel flow is independent from the rest of the domain, both the upper and lower walls are refined and the downstream region is coarsened using a non-conformity except in the near wall region (see figure 9). A particular attention has been paid to the orthogonality of the near wall cells on the hill in order to avoid additional numerical errors close to the wall. The non-dimensional distance to the wall is around 3 in the upstream channel and does not go beyond 7 at the top of the hill during the whole calculation.

Figures 10 and 11 give the velocity profiles at the same locations as in the structured case. The profiles of the previous structured LES are kept for comparison. The results of the LES with a non-conforming mesh are in better agreement with the experiment contrary to the previous calculations. The boundary layer is well predicted compared to the structured calculation (figure 11). However, the profiles seem not fully converged yet. A previous converged calculation on a coarser grid with random inlet boundary conditions (not exposed in the present paper) gave the results shown in figure 12. The velocity profile is in fairly good agreement with the experiment and the present LES should converge to at least the same results. Figure 13 shows the recirculation region in the symmetry plane for both the experiment and the LES on the non-conforming mesh. Although the calculation seems to be not converged in the plane $x=3.69$ downstream the hill, the recirculation region is smooth and seems to be converged. This is probably due to the fact that this region of interest is closer to the hill and characterized by smaller timescales than the far wake. The shallow bubble seems to be reasonably predicted and the re-attachment as well. The reattachment is around $x=2.2$ (in the experimental figure, it is difficult to see the reattachment point). The tangential velocity field in the plane $x=3.69$ is shown in figure 14 (LES field is on the opposite part of the symmetry plane). One can observe a quite flattened vortex similar to that of the experiment The LES shows traces of two vortex cores which may result from a merging of the horseshoe vortex coming from the front and a "wing tip like" wake structure associated with the lift. Longer time averaging could possibly lead to a more complete merging of these two structures. The center of the vortex is located in the (y,z) plane around the point (*1*, *1.7*) which is satisfactory compared to the experimental results and taking into account that no RANS model and no LES on structured meshes managed to predict a similar quality of results. Finally the pressure coefficient is drawn in figure 15. The shape of the curve is correct up to separation thanks to the fine near-wall mesh and inlet conditions but the pressure rises on. The summit is then underestimated, similarly to other LES results obtained by FLOMANIA partners and remains to be explained.

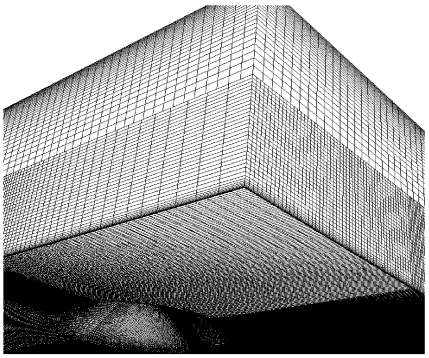

Figure 8: View of the mesh using non-conforming faces

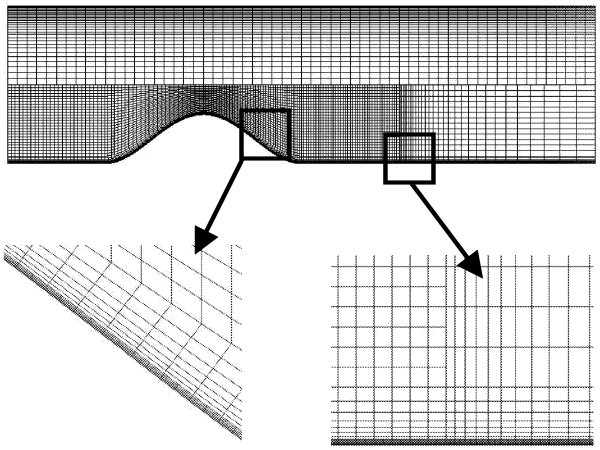

Figure 9: Views of the unstructured mesh using non-conforming faces (symmetry plane *z=0*)

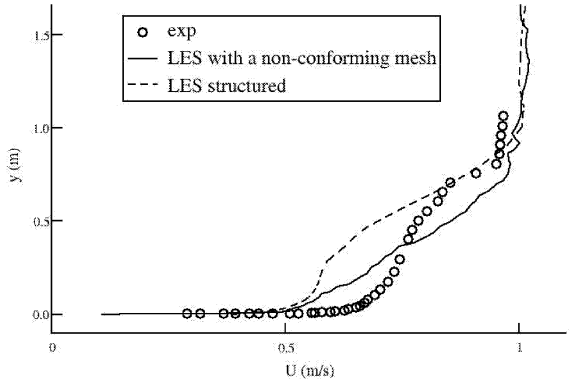

Figure 10: Streamwise velocity profile (*x=3.69, z = 0.08*)

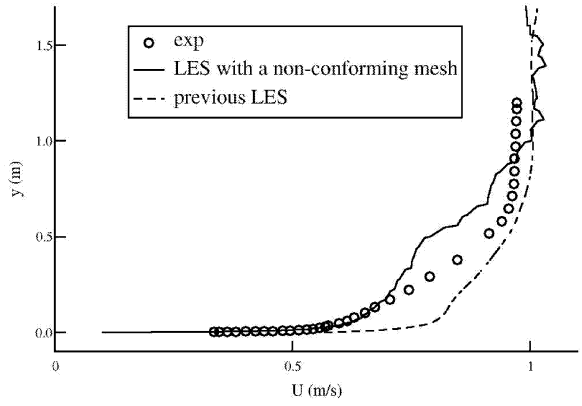

Figure 11: Streamwise velocity profile (*x=3.69, z = 0.8*)

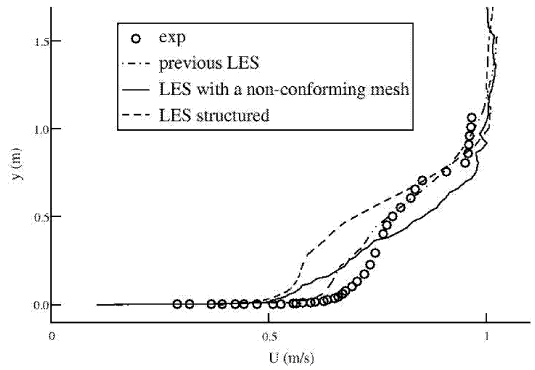

Figure 12: Streamwise velocity profile (*x=3.69, z = 00.8*), comparison with previous converged LES calculation

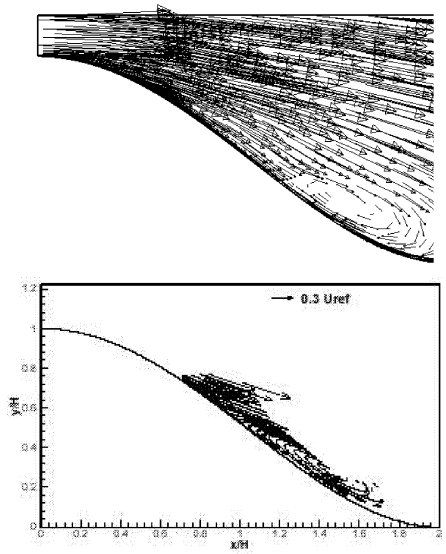

Figure 13: Velocity field in the plane *z=09* (top: LES on a non-conforming mesh, bottom: experiment)

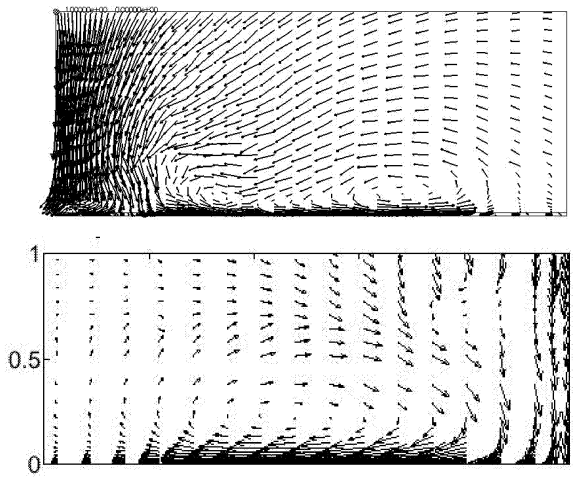

Figure 14: Tangential velocity field in the plane *x=3.69* (top: LES, bottom: experiment with x axis reversed)

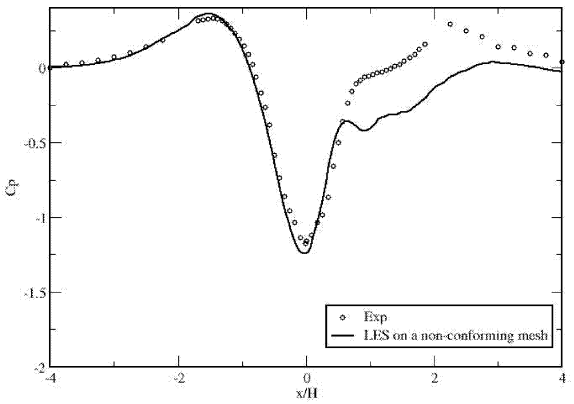

Figure 15: Pressure coefficient along the symmetry plane (z=0)

CONCLUSION

Two RANS models, the *v2-f* in its φ version and the *k-ω* one have been tested on a structured mesh and failed in predicting the 3D hill flow of Simpson et al. (2002). The unsteady LRR model and Large Eddy Simulation are performed on the same meshes and the unsteady RANS approach exhibits a better behavior than LES but is still far from experimental results.

Large Eddy Simulation is then performed on a non-conforming mesh thanks to the unstructured capabilities of *Saturne* code. This mesh has almost the same number of cells as in the structured case. Although the variables are not converged yet, the results are in fairly good agreement with the experimental data concerning the qualitative aspects (recirculation bubble due to the detachment at the hill and the two counter-rotating vortices in a measurement plane). The calculation has still to converge and more comparisons will be done for other quantities like the other velocity components and the Reynolds stresses.

The capability of non-conforming meshes is clearly shown in this paper. Although more numerical investigations have to be performed concerning some particular point, this method will allow as in a next future to handle more industrial applications (at higher Reynolds numbers) with reasonable numbers of grid-points.

ACKNOWLEDGEMENTS

S. Benhamadouche and D. Laurence want to acknowledge the European project Desider Project (Detached Eddy Simulation for Industrial Aerodynamics) which is a collaboration between Alenia, ANSYS–AEA, Chalmers University, CNRS–Lille, Dassault, DLR, EADS Military Aircraft, EUROCOPTER Ger-many, EDF, FOI–FFA, IMFT, Imperial College London, NLR, NTS, NUMECA, ONERA, TU Berlin, and UMIST. The project is funded by the European Community represented by the CEC, Research Directorate–General, in the 6th Framework Programme, under Contract No. AST3-CT-2003-502842.

REFERENCES

Archambeau, F. Méchitoua, N. and Sakiz, M. Code_Saturne : a finite volume code for the computation of turbulent incompressible flows – industrial applications. *Int. J. on Finite Volumes*. 2004.

Benhamadouche, S. and Laurence, D. LES, Coarse LES, and Transient RANS Comparisons on The Flow Across Tube Bundle, *Int. J. Heat and Fluid Flow*, 4, pp 470-479, 2003.

Benhamadouche, S., Mahesh, K. and Constantinescu, G., Colocated finite-volume Schemes for Large-Eddy Simulation on Unstructured Meshes, *Proceedings of the Summer Program*, Center for Turbulence Research, NASA Ames/Stanford Univ., pp 143-154, 2002.

Benhamadouche, S., Sakiz, M., Peniguel, C. and Stephan, J. M., Presentation of New Methodology of Chained Computations using Instationary 3D Approaches in a T-junction of a PWR Nuclear Plant, *17th I. C. on Structural Mech. in Reactor Technology*, Aug. pp17-22, Prague, 2003.

Byun, G., Simpson, R.L. and Hong, C.H. "A study of vortical separation from three-dimensional symmetric bumps", *AIAA Journal*, 42(4):754-765, 2004.

Kim, J., Moin, J. K. P. and Moser R., Turbulence Statistics in Fully Developed Channel Flow at Low Reynolds Number. *J. Fluid Mech.* Vol 177, pp. 133-166, 1987.

Launder B.E., Reece G. J. And Rodi W. Progress in the development of a Reynolds stress turbulence closure. *J. Fluid Mech*, **68**, 231-239, (1975).

Laurence D.R., Uribe, J.C., Utyuzhnikov, S.V. "A robust formulation of the v2f model" Flow, Turbulence and combustion 73: 169-185, 2004.

N. Jarrin, S. Benhamadouche, Y. Addad, D. Laurence, Synthetic turbulence inflow condition for large-eddy simulation, *Turbulence, Heat and Mass Transfer 4*, Antalya, Turkey (2003), *to appear in Progress in Computational Fluid Dynamics (2005)*

Lund, T.S. Generation of Turbulent Inflow Data for Spatially-Developing Boundary Layer Simulations, *Journal of Computational Physics*, 140, 233-258 (1998)

Rhie C.M. and Chow W.L. A numerical study of the turbulent flow past an isolated airfoil with training edge separation. *AIAA Journal,* 21(11):1525-1532, 1983

Simpson, R.L, Hong, C.H. and Byun, G. "A study of vortical separation from an axisymmetric hill", *Int. J. of Heat and Fluid Flow*, 23:582-591, 2002.

Wang C., Jang Y. J. and Leschziner M. A. "Modelling two- and three-dimensional separation from curved surfaces with anisotropy-resolving turbulence closures" , Int. J. of Heat and Fluid Flow, 25, 499-512, 2004

Wilcox, D. C. "Re-assessment of the scale-determining equation for advanced turbulence models" AIAA journal, Vol 26, No11, pp 1299-1310, 1988